


Spectral Analysis of Solar and Geomagnetic Parameters in Relation to Cosmic-ray Intensity for the Time Period 1965 – 2018

M. Tschla¹ · M. Gerontidou¹ · H. Mavromichalaki¹ 

Received: 9 November 2018 / Accepted: 14 January 2019 / Published online: 29 January 2019
© Springer Nature B.V. 2019

Abstract Spectral analysis of solar and geomagnetic parameters as well as of cosmic-ray intensity was performed aiming to identify possible new periodicities and confirm the well-known ones. Specifically, short-, mid-, and long-term periodicities of these parameters such as sunspot number, Bz-component of the interplanetary magnetic field, geomagnetic Ap index, and cosmic-ray intensity over the time period 1965–2018, covering five solar cycles from Cycles 20 to 24, are presented. For this purpose, two different techniques, fast Fourier transformation and wavelet analysis, have been used in order to ensure accuracy in the frequency values and also their localization in the time series. The periodicities resulting from our comprehensive study, including the well-known 11-year and 27-day periods, the harmonics of the 5.5-year and of the 6-, 9-, and 13.9-day periods, respectively, and the ≈ 1.3 -year and 1.7-year periods, were found in all of the above parameters except for the Bz-component of the interplanetary magnetic field. New periodicities such as the ≈ 10 -month period for sunspot number and cosmic-ray intensity and the ≈ 3 -year period for sunspot number, Ap index, and cosmic-ray intensity, were also determined. Furthermore, the newly introduced splitting of the 27-day periodicity into two adjacent peaks was confirmed in the Fourier spectra of the interplanetary magnetic field and the geomagnetic Ap index. It was concluded that several common periodicities appear in solar activity: the Ap index, and the cosmic-ray intensity. This result, in association with the fact that the spectral behavior of geomagnetic-activity parameters, provides invaluable information about the physical processes involved, and indicates that the Ap index might be used as a suitable index for space-weather forecasting.

Keywords Cosmic-ray intensity · Sunspot number · Periodicities · Geomagnetic indices · Interplanetary magnetic field

✉ H. Mavromichalaki
emavromi@phys.uoa.gr

¹ Nuclear and Particle Physics Department, Faculty of Physics, National and Kapodistrian University of Athens, Zografos, 15784 Athens, Greece

1. Introduction

Galactic cosmic rays (GCRs) are energetic charged particles that originated outside our solar system and have energies in the range of $10^6 - 10^{20}$ eV nucleon⁻¹. These high-energy GCRs travel through the heliosphere, and when they reach the Earth's atmosphere, they trigger particle and electromagnetic cascades, creating a great variety of secondary particles called secondary cosmic rays. An important characteristic of cosmic rays inside the solar cavity is their temporal variability on a wide range of timescales. This temporal variation of cosmic-ray intensity must be due to the interaction of cosmic-ray particles with the interplanetary magnetic field (IMF) that is carried by the solar wind. Moreover, there is a well-known anticorrelation between cosmic rays and solar activity as measured by the sunspot number (SSN). Therefore, the issue that arises is to find out the pattern of the IMF and its flow to determine the temporal and spatial evolution of their configurations and to relate them to cosmic-ray variations.

The availability of continuous measurements of the cosmic-ray intensity (CRI) as registered by the network of neutron monitors (Simpson, 2000) as well as of the solar and interplanetary data allows us to investigate the relationships among cosmic rays, IMF, and solar activity. Although periodicities in CRI have been widely studied by several authors (*e.g.* Kudela, Ananth, and Venkatesan, 1991; Mavromichalaki *et al.*, 2003a, 2003b; Kudela *et al.*, 2010; Chowdhury, Kudela, and Moon, 2016) and in solar and geomagnetic parameters were also reported by many researchers (*e.g.* Paularena, Szabo, and Richardson, 1995; Prabhakaran Nayar *et al.*, 2002; Chowdhury and Dwivedi, 2011; Poblet and Azpilicueta, 2018), it is worthwhile to update the common periodicities for a more extended time period and/or to find new ones.

Valdes-Galicia, Perez-Enriquez, and Otaola (1996) and Mavromichalaki *et al.* (2003b) have reported on a short-term variation of 1.68 years in the CRI observed at the Earth in the neutron monitors' range of energy. This variation might appear as a consequence of phenomena rooted in the solar interior that are related to the emergence and transport of magnetic flux. Recently, Singh and Badruddin (2017) examined the past two solar magnetic cycles (1968–1989 and 1989–2014); they found that in addition to the well-known periodicities, like the 27-day (synodic period), the 154-day (Rieger period), the semi-annual, the annual, the 1.3-year, and 1.7-year period, the first (27-day), second (13.5-day), and third (9.0-day) solar-rotation harmonics in the geomagnetic Ap index are observed consistently; annual and ≈ 1.85 -year variations are also observed. Several significant mid-range periodicities, such as ≈ 175 , 133, 113, 104, 84, and 63 days, are detected in sunspot activity, as reported by Joshi, Pant, and Manoharan (2006). In that study, the spectral analysis of sunspot number, sunspot areas, and solar-flare index during Solar Cycle 23 was presented. An important conclusion was that the periodic variations in the northern and southern hemispheres of the Sun present a kind of asymmetrical behavior, while periodicities of ≈ 175 days and ≈ 133 days are highly significant in the sunspot data of the northern hemisphere.

Additionally, Kudela and Sabbah (2016) studied the quasi-periodic and irregular temporal variability of low-energy cosmic rays from ground-based direct measurements such as neutron monitors and muon detectors. They concluded that wavelet spectra are useful tools for studying the fine structure of quasi-periodic variations and their temporal behavior. Studies dedicated to the periodic behavior of the solar and interplanetary magnetic field have also been reported by several authors (Baranyi and Ludmány, 2003; Chang, 2014), and as Bazilevskaya *et al.* (2014) stated, many features of solar quasi-biennial oscillations (QBOs) with timescales of 0.6–4 years are common to different observations. These features include variable periodicity and intermittence with signs of stochasticity.

For the present spectral analysis, daily and monthly values of the above-mentioned time series of sunspot number, IMF, Ap index, and CRI, covering Solar Cycles 20–24 over 1965 to 2018, have been used. We apply two spectral techniques, the wavelet technique (Torrence and Compo, 1998) and the fast Fourier transformation (Brigham, 1988), in order to define significant periodicities on various timescales. These are separated into short-term (referring to periods from 2 to about 30 days), mid-term (from > 30 days to two years), and long-term (greater than two years) periodicities. A comparison of the results obtained from the two methods of analysis for the different time series is performed and yields interesting conclusions.

2. Data and Analysis Technique

2.1. Data Selection

The present analysis concerns the time period from 1965 until 2018, covering Solar Cycles 20–24. Daily and monthly values from 1 January 1965 to 31 March 2018 of the cosmic-ray data recorded by the Moscow neutron-monitor station (geographical coordinates 55.47°N, 37.32°E, cutoff rigidity 2.43 GV) and corrected for pressure were obtained from the high-resolution Neutron Monitor Database (NMDB) (www.nmdb.eu/nest/). Moreover, daily and monthly values from 1 January 1965 to March 2018 of the sunspot number (SSN) measurements from WDC-SILSO, Royal Observatory of Belgium, Brussels (www.sidc.be/silso/datafiles), have been used. Daily data from 1 January 1965 to 31 March 2018 and monthly data from January 1965 to February 2011 of the geomagnetic Ap index were taken from the National Oceanic and Atmospheric Administration (NOAA) (ftp://ftp.ngdc.noaa.gov/STP/GEOMAGNETIC_DATA/INDICES/KP_AP), while daily data from 1 January 1995 to 31 March 2018 and 27-day data from January 1995 to March 2018 for the Bz-component of the IMF in the Geocentric Solar Magnetospheric (GSM) coordinate system from the NASA Goddard Space Flight Center, Space Physics Data Facility (omniweb.gsfc.nasa.gov/form/dx1.html), were also used. It is noted here that the monthly data of the Ap index and the daily and monthly data of the Bz-component of the IMF refer to shorter time intervals than the other parameters due to the lack of available data covering the rest of the time intervals.

2.2. Methods of Analysis

In order to find possible periodic variations in the examined time series, the fast Fourier transform and the wavelet technique (Torrence and Compo, 1998; Katsavrias, Preka-Papadema, and Moussas, 2012) were applied to the selected time series.

The Fourier transform decomposes a function of time (signal) into the frequencies that make it up. This transform of a function of time itself is a complex-valued function of frequency, whose absolute value represents the amount of that frequency present in the original function, and whose complex argument is the phase offset of the basic sinusoid at that frequency. The Fourier transform is called the frequency domain representation of the original signal. The Fourier analysis indicates that any signal can be analyzed in a sum of trigonometric functions.

The periodogram analysis method developed by Lomb and Scargle (Zechmeister and Kürster, 2009) used in this work is a method of estimating a frequency spectrum, based on

the least-squares fit of sinusoids to data samples, similar to the Fourier analysis and also known as the least-squares spectral analysis (LSSA).

Likewise, the wavelet analysis can decompose any signal into a sum of wavelets that originate from a mother wavelet function. A wavelet is a wave-like oscillation with amplitude that begins at zero, increases, and then decreases back to zero. It can be visualized as a “brief oscillation” like one recorded from a heart monitor. The term wavelet function is used to refer to either orthogonal or non-orthogonal wavelets. The Morlet function, which we use as mother function in this work, is a set of non-orthogonal wavelets and can be used with either the discrete or the continuous wavelet transform. The continuous wavelet transform was used in our case, and the functions that we studied were time series $[x_n]$ with equal time-spacing $[\delta t]$ and $n = 0, \dots, N - 1$.

The Fourier transform of a discrete sequence is known as the discrete Fourier transform (DFT),

$$X_k = \sum_{n=0}^N x_n e^{-2i\pi kn/N}. \tag{1}$$

The wavelet transform of the discrete sequence x_n is defined as the convolution of x_n with a scaled and translated version of the mother wavelet function, which is denoted as $\psi(\frac{t}{s})$. The term t denotes time and the term s , called scale, denotes a time interval or a period. Convolution is a mathematical operation on two functions to produce a third one. This operation includes shifting of the first function along the second one, producing integral values of the point-wise multiplication of the two functions. These values define the third function. The wavelet technique is based on this operation. Wavelets with different scales are shifting along the time series, and wherever in the time series the integral value is high, the specific scale or period is considered to have occurred.

More specifically, a version of the convolution theorem states that the convolution of two functions f and g equals the inverse Fourier transform of the point-wise product of Fourier transforms,

$$f * g = F^{-1} \{ F\{f\} \cdot F\{g\} \}, \tag{2}$$

where the asterisk denotes convolution and the dot denotes multiplication.

This version is applied to the continuous wavelet transform of x_n as given by

$$W_n(s) = \sum_{k=0}^{N-1} X_k \psi^*(s\omega_k) e^{i\omega_k n \delta t}, \tag{3}$$

where the angular frequency is defined as $\omega_k = \begin{cases} \frac{2\pi k}{N\delta t}, & k \leq N/2 \\ -\frac{2\pi k}{N\delta t}, & k > N/2 \end{cases}$ and s is the scale, X_k is the discrete Fourier transform of x_n , $\psi(s\omega_k)$ is the Fourier transform of $\psi(\frac{t}{s})$, and the asterisk denotes the complex conjugate.

By varying the wavelet scale $[s]$ and translating along the localized time index n , one can construct a picture showing both the amplitude of any features *versus* the scale and how this amplitude varies with time, as is shown in Figures 1, 2, 4, 5, 7, 8, 9, 12, and 13. This is the difference between a wavelet transform and a Fourier transform, which only shows the amplitude of each frequency.

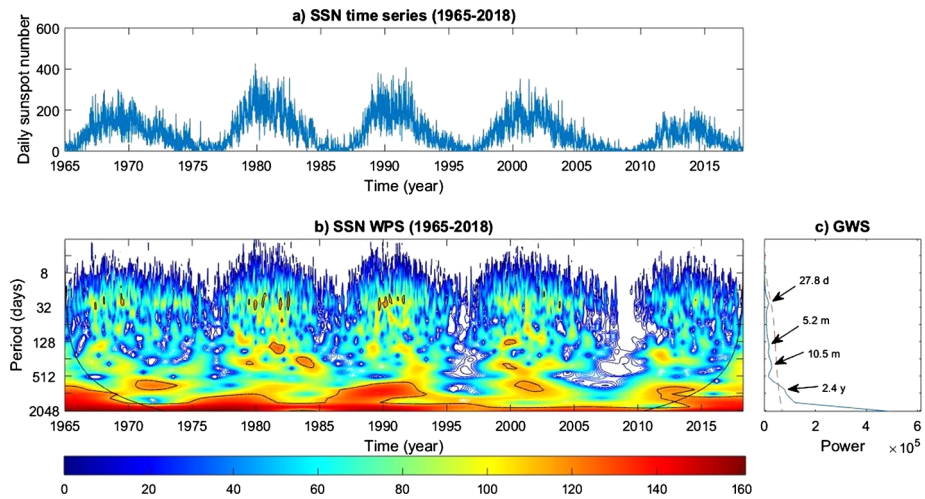


Figure 1 Temporal profile of the daily values of sunspot number (a), the wavelet power spectrum (WPS) (b), and the global wavelet spectrum (GWS) (c) of this parameter in the period range from 2 to 2048 days (lower panels) for the time interval 1965–2018.

3. Results

Applying the two techniques described above to the time series of the sunspot number, the Bz-component of the IMF, the geomagnetic Ap index, and the CRI, a number of diagrams are obtained, of which only those with the best-fit resolution and coherence are cited in this work. Many interesting periodic variations are outlined, giving useful conclusions for space-weather studies.

3.1. Sunspot Number

The wavelet analysis applied on the daily values of the sunspot-number time series gave a number of short-, mid-, and long-term periodicities that we list in Table 2, and the corresponding diagrams are presented in Figure 1. In the upper panel of this figure the temporal profile of the daily time series displays the well-known 11-year variation. In the lower panel the wavelet power spectrum (WPS) of this parameter in the range of 2–2048 days is illustrated, while in the right panel the global wavelet spectrum (GWS) of the sunspot number is illustrated. The periodicities that we are interested in are those corresponding to the peaks in the GWS. The 95% confidence level is indicated by the thick black contours in WPS and by the dashed red curve in the GWS. In this figure, the 27-day, 5.2-, 10.5-month, and 2.4-year periodicities are obvious. The well-known 27-day periodicity is due to the rotation of the Sun. The 5.2-month periodicity, known as the Rieger period, often appears during the maximum of the solar cycle (Rieger *et al.*, 1984). It is caused by the strong magnetic field that is generated in the convection zone of the Sun and is driven outward, causing temporal distributions of various parameters in the interplanetary medium. For this reason, we detect an integral multiple of that periodicity in the CRI. The 10.5-month and 2.4-year periodicity belong to the QBOs, which cover a wide temporal interval of 0.6–4 years. These are well-known variations in solar activity, interplanetary parameters, geomagnetic indices, and CRI (Bazilevskaya *et al.*, 2014). The QBOs are considered as one of the basic variations of solar-activity indices on scales shorter than 11 years, and they are probably intrinsic properties

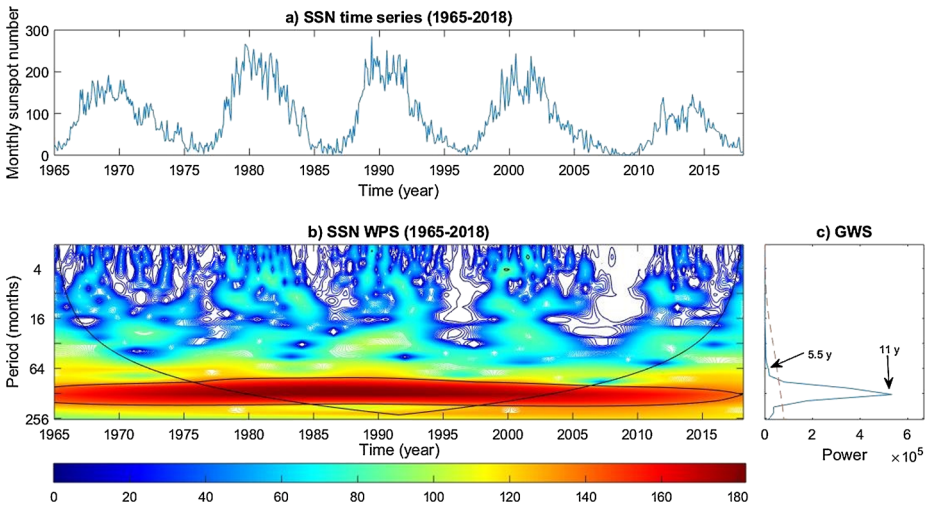


Figure 2 Temporal profile of the monthly values of the sunspot number (a), the wavelet power spectrum (WPS) (b) and the global wavelet spectrum (GWS) (c) of this parameter in the period range from 2 to 256 months (*lower panels*) for the time interval 1965–2018.

of the Sun related to the solar-dynamo mechanism (Chowdhury, Kudela, and Moon, 2016). We note that the Rieger and the 10.5-month period are stronger in Solar Cycles 21 and 23, and the 2.4-year period is stronger in Solar Cycles 20, 22, and 24. So, we are driven to the conclusion, which has also been noted in previous works, that odd and even cycles have characteristics in common (Otaola, Perez-Enriquez, and Valdes-Galicia, 1985; Mavromichalaki, Marmatsouri, and Vassilaki, 1988; Durney, 2000; Yoshida, 2014). This is because the polarity of the solar magnetic field reverses every 11 years around the maximum of the solar cycle, causing the 22-year magnetic cycle (Mavromichalaki, Belehaki, and Rafios, 1998; Mavromichalaki *et al.*, 2017). Some phenomena, like these periodicities, therefore follow a 22-year periodicity, and this is why specific works divide the time periods into magnetic cycles (Singh and Badruddin, 2017).

Moreover, the wavelet technique applied to the monthly values of the sunspot-number time series presented the same periodicities as above, as shown in Figure 2. The WPS clearly indicates the 11-year solar cycle and its second harmonic 5.5-year periodicity caused by the enhanced power of the second harmonic that arises from the asymmetric nature of the solar cycle (Currie, 1976; Sugiura, 1980; Mursula, Usoskin, and Zieger, 1997). As we see subsequently, the fast Fourier transform also includes in the spectrum the multiples and submultiples of the dominant frequencies.

The Lomb–Scargle power spectrum of the sunspot-number time series obtained from the fast Fourier analysis is depicted in Figure 3. The noted peaks are above the 95% confidence level and are given in Table 1. In addition to the above periodicities obtained from the wavelet analysis, there is a 1.1-year periodicity that is related to the Earth’s orbit around the Sun, and 1.9-, 3.2-, and 3.9-year periodicities that belong to the QBOs. Moreover, there is a 6.5-year periodicity that may be explained as the third harmonic of the magnetic cycle. The difference from the wavelet analysis is that Fourier analysis gives a better estimate of the frequency components, but the advantage of the wavelet analysis is that we can define the time interval in which the specific frequency has occurred, and we can also come to conclusions

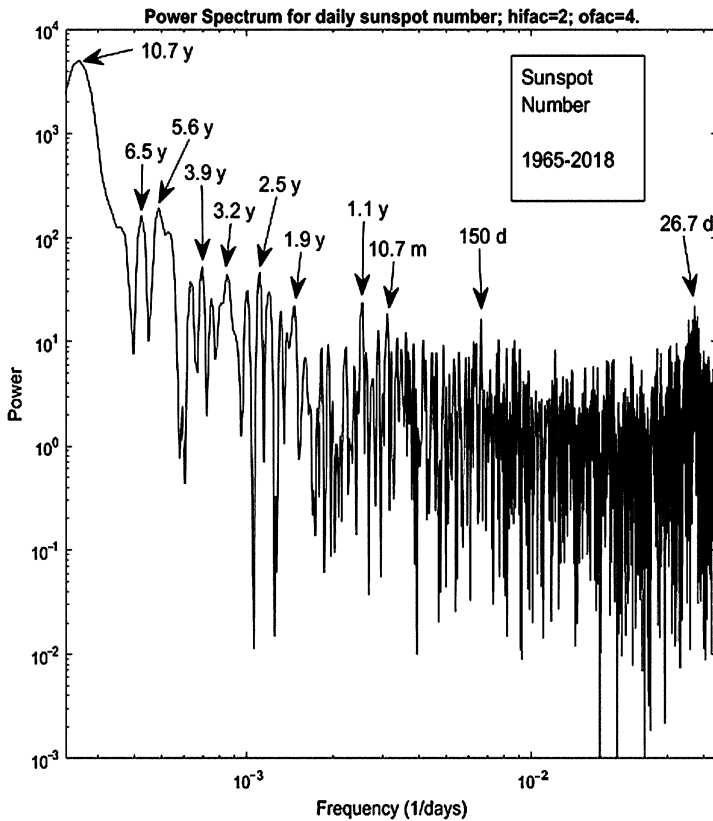


Figure 3 Lomb–Scargle power spectrum of the daily sunspot-number time series during the interval 1965–2018.

such as the common characteristics between odd and even solar cycles (Mavromichalaki, Marmatsouri, and Vassilaki, 1988).

3.2. Interplanetary Magnetic Field

The WPS obtained from the daily values of the IMF Bz-component is shown in Figure 4, while the resulting periodicities are illustrated in Table 2. It depicts the 13.9- and 27-day periodicities as being the most powerful ones for this parameter, while the rest of them are far below the 95% confidence level indicated by the dashed line. In the WPS of the monthly values of the Bz-time-series, which is depicted in Figure 5, we detect the 2.2- and 3.7-month periodicities above the 95% confidence level. We also detect the 1-year periodicity, which is right below the 95% confidence level, and the 4.1- and 8.2-year periodicities, which are far below this confidence level. In the Lomb–Scargle power spectrum of the Bz-time-series that is shown in Figure 6, the resulting periodicities that are above the 95% confidence level are at 14.1 and 28.5 days.

It is interesting to note here that our analysis shows that the 27-day periodicity as well as its second harmonic are split into two peaks. This implies that the Bz-component of the IMF as measured at the near-Earth environment is slightly variable. This is why the peak is not narrow and well defined. Chang (2014) indicated that a fundamental period

Table 1 Significant peaks from the Lomb–Scargle analysis of the daily values of the sunspot number, Bz, geomagnetic Ap index, and CRI time series during the interval 1965–2018.

Fast Fourier Transform (FFT) (Lomb–Scargle)				
Confidence level 95%				
Periodicities	SSN	IMF Bz	Ap index	CRI
Short-term	–	–	9 d,	–
	–	14.1 d	13.5 d	–
	26.7 d	28.5 d	25.3 d	–
Mid-term	5 m	–	6.1 m	–
	10.7 m	–	8.7 m	9.5 m
	1.1 y, 1.9 y	–	1.3 y, 1.7 y	1.2 y, 1.7 y
Long-term	2.5 y	–	2.3 y	–
	3.2 y	–	3 y	3 y
	–	–	3.6 y	3.7 y
	3.9 y	–	4 y	–
	5.6 y	–	5.2 y	5 y
	6.5 y	–	–	7.2 y
	10.7 y	–	10.6 y	10.5 y
	–	–	–	19 y

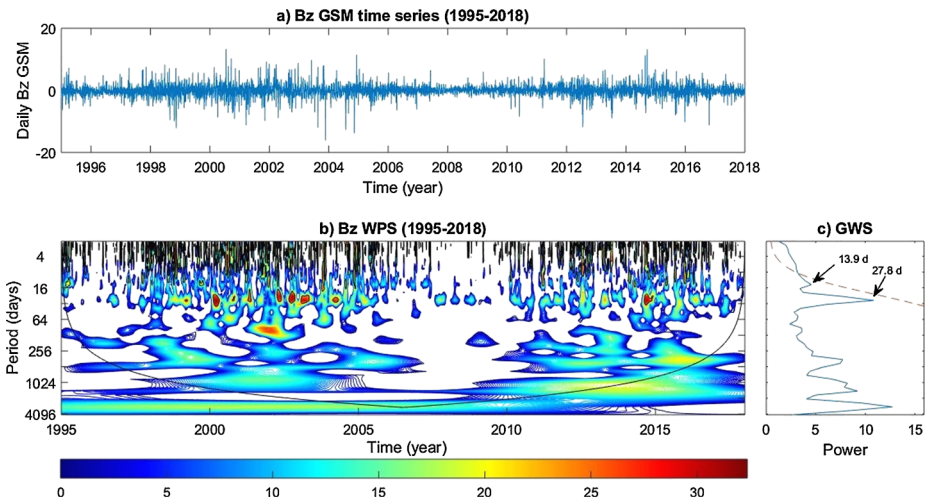


Figure 4 Temporal profile of the daily values of the Bz-component of IMF (a), the wavelet power spectrum (WPS) (b), and the global wavelet spectrum (GWS) (c) of this parameter in the period range from 2 to 4096 days (lower panels) for the time interval 1995–2018.

may cause sidelobes around the dominant 27-day periodicity, and therefore the peak is split. Specifically, he implemented a straightforward model of an oscillation frequency modulated by an arbitrary agent and found that this arbitrary agent is the one-year period. This result agrees with our result of a one-year periodicity that is just below the 95% confidence level in Figure 5 (Baranyi and Ludmány, 2003). According to Poblet and Azpilicueta (2018), the

Table 2 Significant peaks from the wavelet analysis in sunspot number, Bz, geomagnetic Ap index, and CRI during the interval 1965–2018.

Wavelet Analysis				
Periodicities	SSN	IMF Bz	Ap index	CRI
Short-term	–	–	6.9 d	–
	–	–	–	–
	–	13.9 d	11.7 d	–
	27.8 d	27.8 d	27.8 d	–
Mid-term	–	2.2 m, 3.7 m	–	–
	5.2 m	–	6.2 m	–
	10.5 m	–	–	–
	–	1 y	1.2 y	1.7 y
Long-term	2.4 y	–	–	–
	–	–	–	2.9 y
	–	–	–	–
	5.5 y	–	–	–
	11 y	–	11 y	11 y
	–	–	–	18.5 y

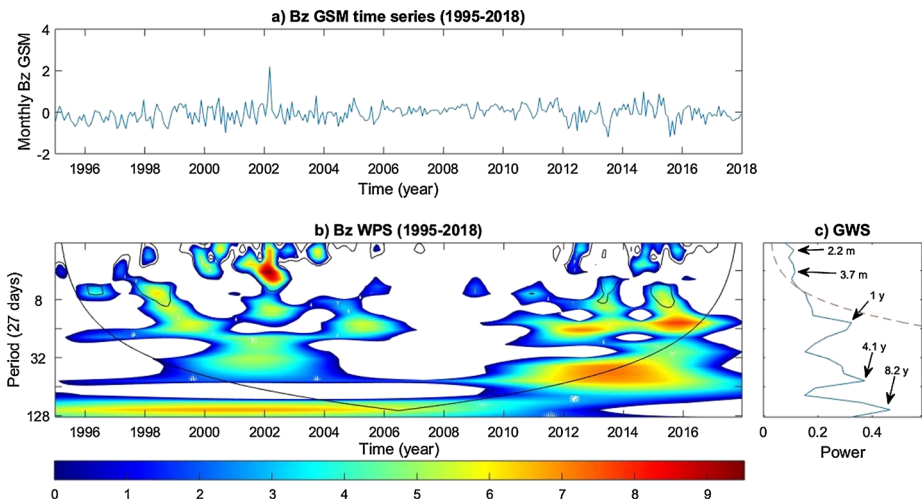


Figure 5 Temporal profile of the monthly values of the Bz-component of IMF (*upper panel*), the wavelet power spectrum (WPS) and the global wavelet spectrum (GWS) of this parameter in the period range from 2 to 128 months (*lower panels*) for the time interval 1995–2018.

physical process responsible for the 27-day signal in the magnetic activity is related to the solar wind and not to the solar electromagnetic radiation.

It is interesting to note that in this work a similar splitting was found also in the Lomb–Scargle power spectrum of the geomagnetic Ap index depicted below in Figure 11. It is noted that this splitting does not appear in the sunspot-number and CRI power spectra.

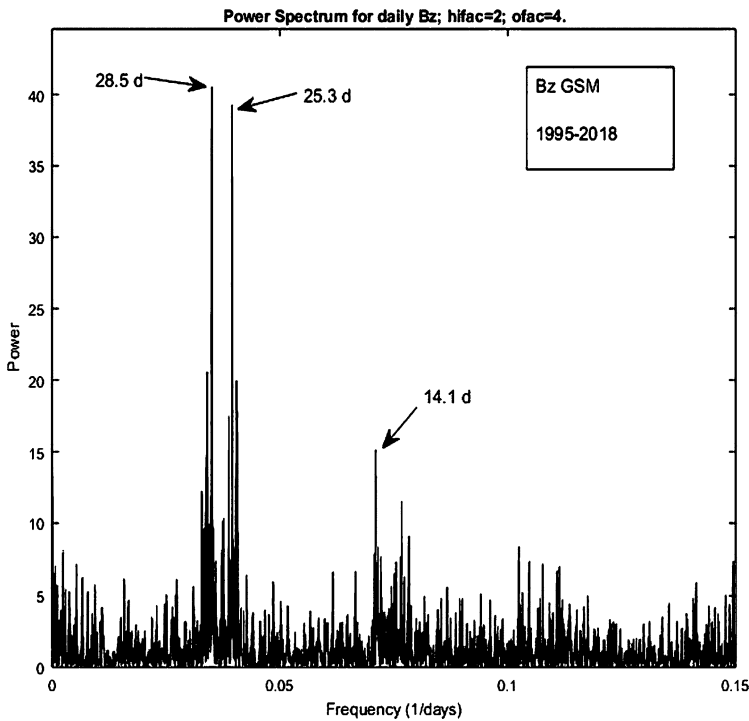


Figure 6 Lomb–Scargle power spectrum of the Bz-GSM time series during 1995–2018.

3.3. Geomagnetic Ap Index

The WPS of the daily time series of the geomagnetic Ap index is depicted in Figure 7, and it shows the first, second, and third harmonic of the 27-day rotational period, the 6-month periodicity that is well known for the Ap index, and the 1.2-year periodicity, which both belong to QBOs (Paularena, Szabo, and Richardson, 1995). The first and second harmonics of the 11-year solar cycle can also be observed in Figure 9, which also depicts the WPS of the daily time series of the geomagnetic Ap index in a different time range. The WPS of the monthly time series of the Ap index is depicted in Figure 8 and shows the semi-annual periodicity and the 11-year solar cycle. We observe that the GWS of the Ap index is clear and smoother than those of the other parameters.

The Lomb–Scargle power spectrum of the Ap index is shown in Figure 10. In addition to the periodicities from WPS, 1.3- and 1.7-year periodicities are also present, and they are considered to be multiples of the Rieger period. Moreover, 2.3-, 3-, 3.6-, and 4-year periodicities are depicted and belong to QBOs. These periodicities are similar to those of the sunspot number because the solar disturbances are transferred to the heliosphere through the open magnetic flux or solar wind and are detected in heliospheric and magnetospheric parameters and in CRI, as we show below. In addition to these periodicities, the splitting of the 27-day periodicity into two peaks, as was mentioned above, is also depicted in Figure 10. For a better understanding, this splitting is shown separately in Figure 11.

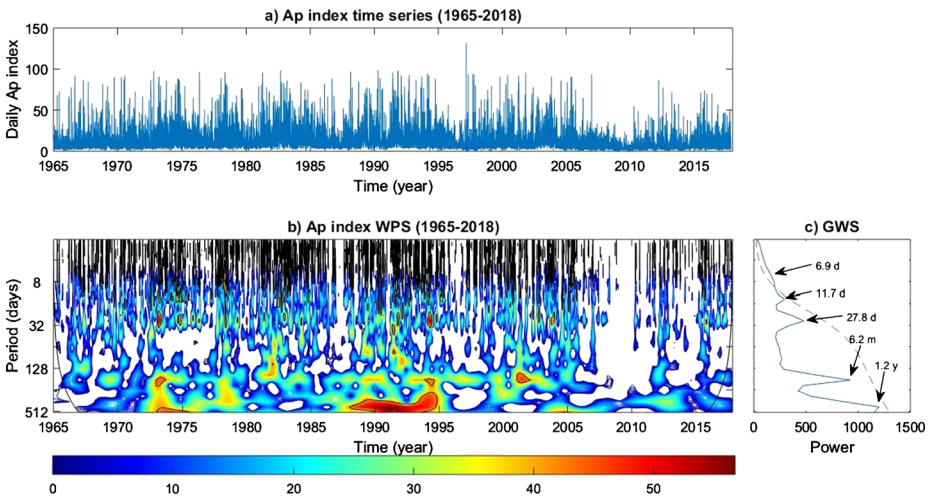


Figure 7 Temporal profile of the daily values of the geomagnetic Ap index (a), the wavelet power spectrum (WPS) (b), and the global wavelet spectrum (GWS) (c) of this parameter in the period range from 2 to 512 days (*lower panels*) for the time interval 1965–2018.

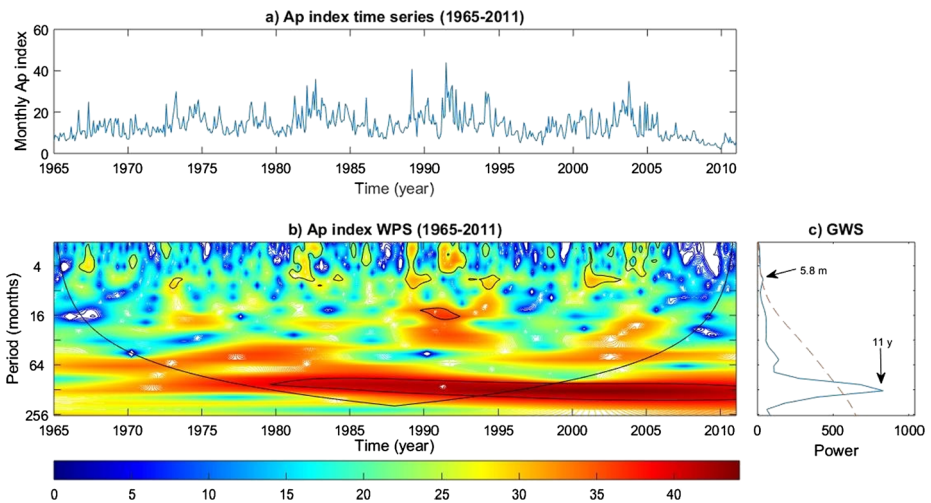


Figure 8 Temporal profile of the monthly values of the geomagnetic Ap index (a), the wavelet power spectrum (WPS) (b), and the global wavelet spectrum (GWS) (c) of this parameter in the period range from 2 to 256 months (*lower panels*) for the time interval 1965–2011.

3.4. Cosmic-ray Intensity

The WPS of the daily time series of the CRI is shown in Figure 12. In these time series, the 1.7- and 2.9-year periodicities are observed. The 1.7-year periodicity is an integral multiple of the Rieger period, while the 2.9-year periodicity belongs to the QBOs, as has already been mentioned in the sunspot-number section. The differences between odd and even cycles (Otaola, Perez-Enriquez, and Valdes-Galicia, 1985) regarding periods shorter than three

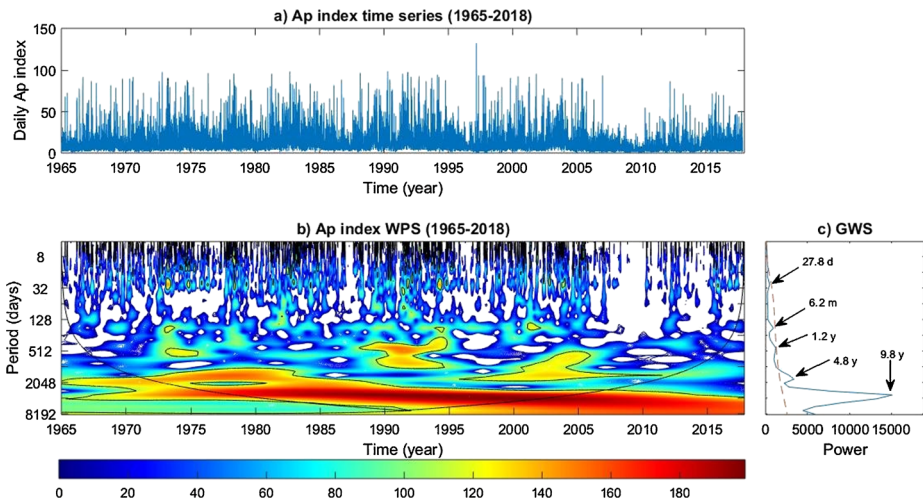


Figure 9 Temporal profile of the daily values of the geomagnetic Ap index (a), the wavelet power spectrum (WPS) (b), and the global wavelet spectrum (GWS) (c) of this parameter in the period range from 4 to 8192 days (lower panels) for the time interval 1965–2018.

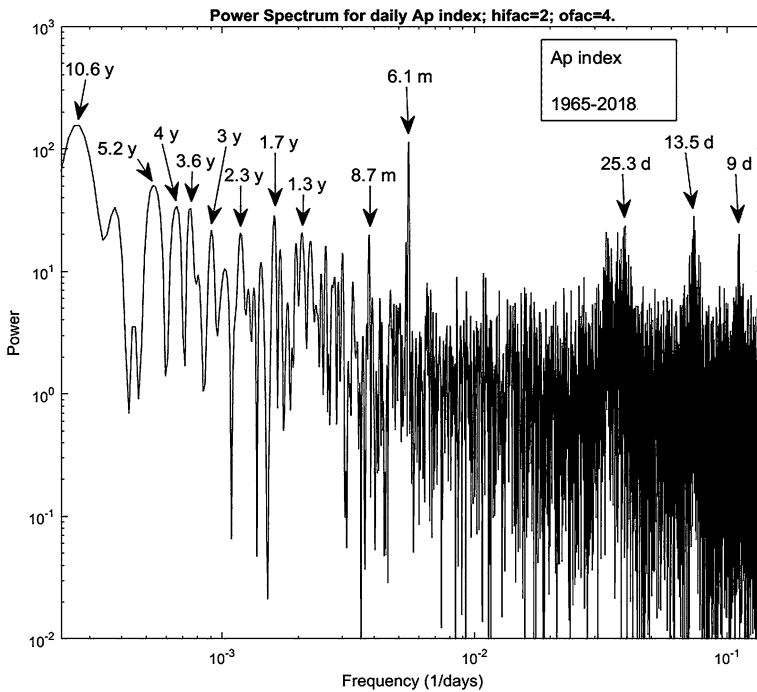


Figure 10 Lomb–Scargle power spectrum of the geomagnetic Ap index time series during the interval 1965–2018.

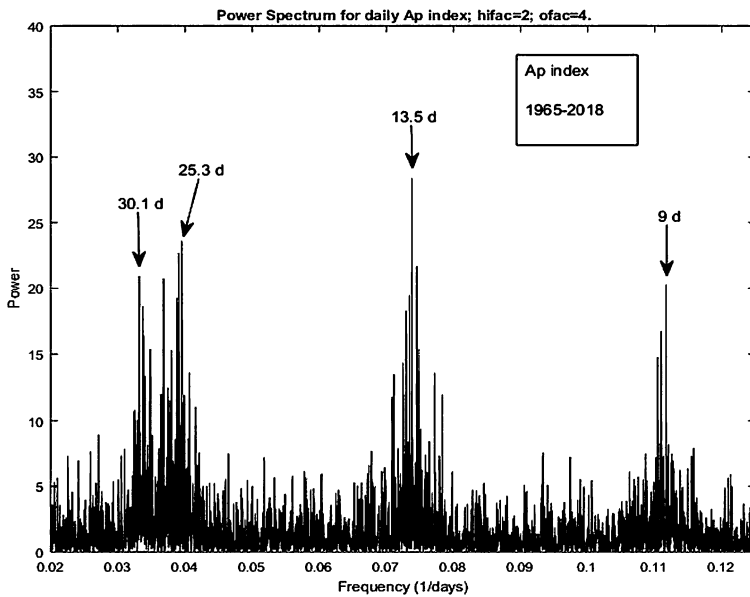


Figure 11 Lomb–Scargle power spectrum of the geomagnetic Ap index time series indicating the splitting of the 27-day periodicity during 1965–2018.

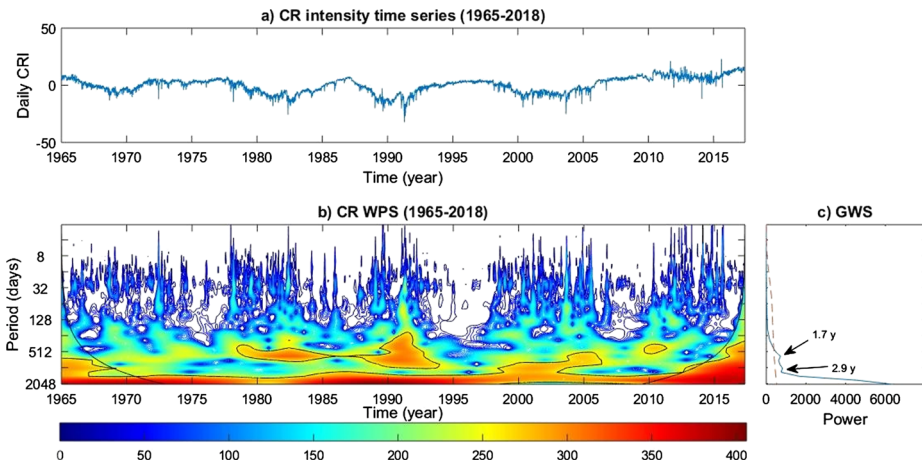


Figure 12 Temporal profile of the daily values of the cosmic ray intensity (a), the wavelet power spectrum (WPS) (b), and the global wavelet spectrum (GWS) (c) of this parameter in the period range from 2 to 2048 days (lower panels) for the time interval 1965–2018.

years are not so clear as in the WPS of the solar activity because the long-term periodicities are much more powerful than the short-term ones, leading to the latter being overshadowed.

In addition, the WPS of CRI for the monthly time series is shown in Figure 13. In addition to the solar-cycle variation, the periodicity of 18.5 years of the magnetic cycle inside the cone of influence is observed. Note here that this periodicity appears only in the CRI and

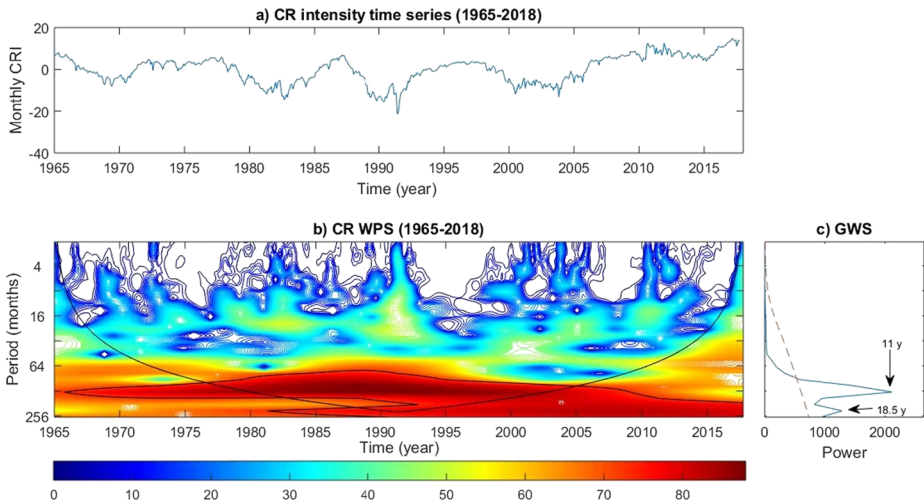


Figure 13 Temporal profile of the monthly values of the cosmic-ray intensity (a), the wavelet power spectrum (WPS) (b), and the global wavelet spectrum (GWS) (c) of this parameter in the period range from 2 to 256 months (lower panels) for the time interval 1965–2018.

not for the rest of the parameters. This confirms the direct connection between magnetic field and CRI.

The periodicities that are mentioned earlier in the sunspot number and geomagnetic Ap index are also present in the Lomb–Scargle power spectrum of the CRI, as shown in Figure 14. In addition to the CRI periodicities from WPS, in this figure we also detect 9.5-month, 1.1-year, and 7.2-year periodicities. The 1.1-year periodicity is due to the Earth’s orbit around the Sun, and the 7.2-year periodicity is probably related to the magnetic cycle as its third harmonic.

A summary of the periodicities that we have found for the four time series using fast Fourier and wavelet analysis on a daily and monthly basis are given in Tables 1 and 2, respectively.

4. Conclusions

We studied periodicities on various timescales such as short-, mid-, and long-term periodicities that are detected in the solar sunspot activity, the Bz-component of the IMF, the geomagnetic Ap index, and the CRI. This study extends from 1965 to 2018, covering a long time interval of 53 years, comprising Solar Cycles 20 to 24. Two different techniques of analysis, the fast Fourier Transform and the wavelet analysis, were applied to the above-mentioned parameters in order to define their significant periodicities. Several periodicities resulting from previous studies are confirmed, and new periodicities are determined. The result of Chang (2014) of the splitting of the 27-day periodicity in the Bz-component of the interplanetary magnetic field has been confirmed as well, and this splitting is noted also for first time in this work in the geomagnetic Ap index.

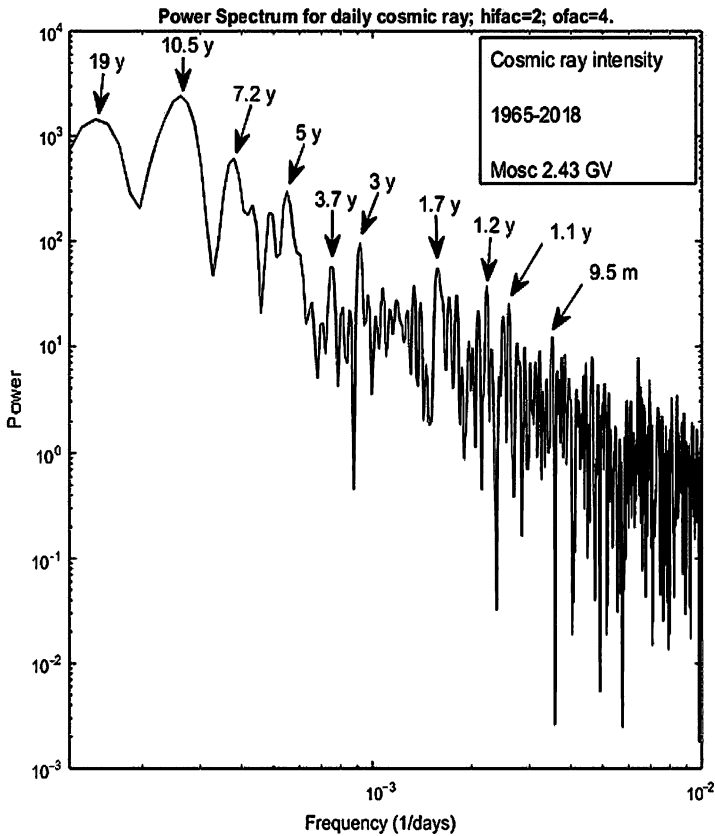


Figure 14 Lomb–Scargle power spectrum of CRI time series during 1965–2018.

More specifically, the following main conclusions have been obtained:

a) Long-term Periodicities

The long-term periodicity of 11 years appears to exist in the examined parameters SSN, geomagnetic Ap index, and CRI in both techniques, as expected (Forbush, 1954). In the case of the Bz-component of the IMF, this variation is not clear.

In our examined period covering five solar cycles (Cycles 20–24), the well-known periodicity of 22 years found in the CRI (Mavromichalaki *et al.*, 2003b) seems to appear with a value of ≈ 19 years and denotes the direct relationship of the CRI with solar activity. As was pointed out by Mavromichalaki *et al.* (2003b), this periodicity is associated with the magnetic cycle due to the solar magnetic-polarity reversal. Moreover, the ≈ 7 -year periodicity found in SSN and CRI time series appears to be related to the 22-year cycle, being its third harmonic. The ≈ 2.4 -year period in the SSN and in the Ap-index, the 3-year period in SSN, Ap index, and CRI, the ≈ 3.6 -year period in Ap and CRI, and the ≈ 4 -year period in SSN and Ap are new periodicities determined in this work.

b) Mid-term Periodicities

The observed mid-term periodicities of ≈ 1.3 years and 1.7 years, found in all of the above parameters except for the Bz-component of IMF, are integral multiples of the Rieger period. The 1.3-year periodicity in the geomagnetic Ap index was also found by Paularena,

Szabo, and Richardson (1995), while the 1.7-year periodicity in CRI was determined by Valdes-Galicia, Perez-Enriquez, and Otaola (1996).

The fundamental periods, like the five-month period known as the Rieger period and the semi-annual period, appear only in the SSN and the Ap index. These results are consistent with those of previous works (Rieger *et al.*, 1984; Prabhakaran Nayar *et al.*, 2002; Baranyi and Ludmány, 2003; Joshi, Pant, and Manoharan, 2006; Chowdhury and Dwivedi, 2011; Bazilevskaya *et al.*, 2014).

We can note here that in addition to the above-mentioned variations, many other periodicities that to our knowledge have not been defined before were determined here. The 2.2- and 3.7-month periodicity in the IMF Bz, the 9.5-month in the CRI, and the ≈ 10.6 -month and the 1.9-year periodicities in SSN are new periodicities determined in this work.

c) Short-term Periodicities

The short-term periodicity of 27 days, due to the solar rotation, is revealed by both techniques in the parameters SSN, Bz, and Ap. This result is in agreement with the results found by Joshi, Pant, and Manoharan (2006), Chang (2014), Singh and Badruddin (2017), Poblet and Azpilicueta (2018), and others.

It is worthwhile to mention that although the 27-day fluctuation in CRI is detected, it is not observed in the corresponding figures because the CRI power of the long-term 11-year periodicity much larger than the power of the 27-day periodicity. We note that many works, such as those by Kudela, Ananth, and Venkatesan (1991), Mavromichalaki *et al.* (2003b), Chowdhury, Kudela, and Moon (2016), are based on the detection of the 27-day periodicity in CRI recorded by neutron monitors. This periodicity is not easy to determine in the CRI power spectrum of our analysis because together with the short- and mid-term periodicities, the long-term periodicities are simultaneously analyzed, being much more powerful than the short-term ones. Moreover, this period due to the synodic rotation period of the Sun is not directly connected with the modulation of the CRI, and thus it is not shown in the spectral analysis of long-time periods.

Moreover, we detect a splitting in the 27-day peak in the Fourier power spectrum of the Bz-component of the IMF and the Ap index. This result is also emphasized in the work of Chang (2014), indicating that a long-term variation may cause a splitting in the principal peak of the 27-day periodicity because in the power spectrum of geomagnetic-activity indices, the 27-day peak is frequency-modulated by the periodic one-year variation. It is noted here that the \approx one-year variation is already found in this work for both parameters by the two techniques.

Furthermore, all short- and mid-term periodicities of the Ap index as shown in the global wavelet spectrum from the wavelet analysis are smooth and clear during the examined period (Singh and Badruddin, 2017). Together with the presence of the solar-rotation harmonics at 9 and 13.5 days in the global wavelet spectrum, this establishes the geomagnetic Ap index as a suitable index for space-weather monitoring (Baker, 1998). Currently, many space-weather forecasting centers use this parameter as an indicator of space-weather conditions issued in daily forecasting reports (spaceweather.phys.uoa.gr).

Finally, based on the obtained wavelet power spectra of the four parameters examined here, we can outline that the maximum and the declining phases of the solar cycles are characterized by the most significant periodicities, and so they are the most appropriate time periods for the study of short- and mid-term variations. This research can be useful to the scientific community for the monitoring of many space-weather effects and applications.

Acknowledgements We gratefully acknowledge the wavelet software provided by C. Torrence and G. Compo (paos.colorado.edu/research/wavelets/) and the Neutron Monitor Database-NMDB, funded under

the European Union's FP7 Program (contract no. 213007). We acknowledge the National Geophysical Data Centre-NOAA, the World Data Center of Kyoto, the Sunspot Index and Long-term Solar Observations-SILSO, and the OMNIWeb of the NASA Goddard Space Flight Center. Thanks are also due to C. Katsavrias and to the anonymous reviewer for suggestions that significantly improved this work.

Disclosure of Potential Conflicts of Interest The authors declare that they have no conflicts of interest.

Publisher's Note Springer Nature remains neutral with regard to jurisdictional claims in published maps and institutional affiliations.

References

- Baker, D.N.: 1998, What is space weather? *Adv. Space Res.* **22**, 7. DOI.
- Baranyi, T., Ludmány, A.: 2003, Semiannual behavior of monthly mean of B_z component of geoeffective ($K_p > 3$) coronal mass ejections, Solar variability as an input to the Earth's environment. In: Wilson, A. (ed.) *Proceedings of ICSC 2003 – Solar Variability as an Input to the Earth's Environment SP-535*, ESA, Noordwijk, 563. ISBN 92-9092-845-X.
- Bazilevskaya, G., Broomhall, A.M., Elsworth, Y., Nakariakov, V.M.: 2014, A combined analysis of the observational aspects of the quasi-biennial oscillation in the solar magnetic activity. *Space Sci. Rev.* **186**, 359. DOI.
- Brigham, E.O.: 1988, *The Fast Fourier Transform and Its Applications*, Prentice-Hall, Inc., Upper Saddle River. ISBN 0-13-307505-2.
- Chang, H.-Y.: 2014, Frequency-modulated solar rotational periodicity of geomagnetic indices. *Publ. Astron. Soc. Japan* **66**, 86. DOI.
- Chowdhury, P., Dwivedi, B.N.: 2011, Periodicities of sunspot number and coronal index time series during Solar Cycle 23. *Solar Phys.* **270**, 365. DOI.
- Chowdhury, P., Kudela, K., Moon, Y.J.: 2016, A study of heliospheric modulation and periodicities of galactic cosmic rays during Cycle 24. *Solar Phys.* **291**, 581. DOI.
- Currie, R.G.: 1976, Long period magnetic activity – 2 to 100 years. *Astrophys. Space Sci.* **39**, 251. DOI.
- Durney, B.R.: 2000, On the differences between odd and even solar cycles. *Solar Phys.* **196**, 421. DOI.
- Forbush, S.E.: 1954, World-wide cosmic-ray variations, 1937 – 1952. *J. Geophys. Res.* **59**, 525. DOI.
- Joshi, B., Pant, P., Manoharan, P.K.: 2006, Periodicities in sunspot activity during Solar Cycle 23. *Astron. Astrophys.* **452**, 647. DOI.
- Katsavrias, C., Preka-Papadema, P., Moussas, X.: 2012, Wavelet analysis on solar wind parameters and geomagnetic indices. *Solar Phys.* **280**, 623. DOI.
- Kudela, K., Ananth, A.G., Venkatesan, D.: 1991, The low-frequency spectral behavior of cosmic ray intensity. *J. Geophys. Res.* **96**, 15871. DOI.
- Kudela, K., Sabbah, I.: 2016, Quasi-periodic variations of low energy cosmic rays. *Sci. China, Technol. Sci.* **59**, 547. DOI.
- Kudela, K., Mavromichalaki, H., Papaioannou, A., Gerontidou, M.: 2010, On midterm periodicities in cosmic rays. *Solar Phys.* **266**, 173. DOI.
- Mavromichalaki, H., Belehaki, A., Rafios, X.: 1998, Simulated effects at neutron monitor energies: evidence of the 22-year cosmic ray variation. *Astron. Astrophys.* **330**, 764.
- Mavromichalaki, H., Marmatsouri, E., Vassilaki, A.: 1988, Solar-cycle phenomena in cosmic-ray intensity: differences between even and odd cycles. *Earth Moon Planets* **42**, 233. DOI.
- Mavromichalaki, H., Preka-Papadema, P., Liritzis, I., Petropoulos, B., Kurt, V.: 2003a, Short-term variations of cosmic-ray intensity and flare-related data in 1981 – 1983. *New Astron.* **8**, 777. DOI.
- Mavromichalaki, H., Preka-Papadema, P., Petropoulos, B., Tzagouri, I., Georgakopoulos, S., Polygiannakis, J.: 2003b, Low and high frequency spectral behaviour of cosmic ray intensity for the period 1953 – 1996. *Ann. Geophys.* **21**, 1681. DOI.
- Mavromichalaki, H., Preka-Papadema, P., Theothoropoulou, A., Paouris, E., Apostolou, Th.: 2017, A study of the possible relation of the cardiac arrhythmias with the magnetic field polarity reversals. *Adv. Space Res.* **59**, 366. DOI.
- Mursula, K., Usoskin, I., Zieger, B.: 1997, On the claimed 5.5-year periodicity in solar activity. *Solar Phys.* **176**, 201. DOI.
- Otaola, J.A., Perez-Enriquez, R., Valdes-Galicia, J.F.: 1985, Difference between even and odd 11-year cycles in cosmic ray intensity. In: Jones, F.C., Adams, J., Mason, G.M. (eds.) *Proc. 19th ICRC*, **4**, CP-2376, 493. NASA GSFC, Greenbelt.

- Paularena, K.I., Szabo, A., Richardson, J.D.: 1995, Coincident 1.3-year periodicities in the Ap geomagnetic index and the solar wind. *Geophys. Res. Lett.* **22**, 3001. [DOI](#).
- Poblet, F.L., Azpilicueta, F.: 2018, 27-day variation in solar-terrestrial parameters: global characteristics and an origin based approach of the signals. *Adv. Space Res.* **61**, 2275. [DOI](#).
- Prabhakaran Nayar, S.R., Radhika, V.N., Revathy, K., Ramadas, V.: 2002, Wavelet analysis of solar, solar wind and geomagnetic parameters. *Solar Phys.* **208**, 359. [DOI](#).
- Rieger, E., Share, G.H., Forrest, D.J., Kanbach, G., Reppin, C., Chupp, E.L.: 1984, A 154-day periodicity in the occurrence of hard solar flares. *Nature* **312**, 623. [DOI](#).
- Simpson, J.A.: 2000, The cosmic ray nucleonic component: the invention and scientific uses of the neutron monitor. *Space Sci. Rev.* **93**, 11. [DOI](#).
- Singh, Y.P., Badruddin: 2017, Short- and mid-term oscillations of solar, geomagnetic activity and cosmic ray intensity during the last two solar magnetic cycles. *Planet. Space Sci.* **138**, 1. [DOI](#).
- Sugiura, M.: 1980, What do we expect in magnetic activity in the current solar cycle? *Eos Trans. AGU* **61**, 673. [DOI](#).
- Torrence, C., Compo, G.P.: 1998, A practical guide to wavelet analysis. *Bull. Am. Meteorol. Soc.* **79**, 61. [DOI](#).
- Valdes-Galicia, J.F., Perez-Enriquez, R., Otaola, J.A.: 1996, The cosmic-ray 1.68-year variation: a clue to understand the nature of the solar-cycle. *Solar Phys.* **167**, 409. [DOI](#).
- Yoshida, A.: 2014, Difference between even- and odd-numbered cycles in the predictability of solar activity and prediction of the amplitude of cycle 25. *Ann. Geophys.* **32**, 1035. [DOI](#).
- Zechmeister, M., Kürster, M.: 2009, The generalised Lomb–Scargle periodogram. A new formalism for the floating-mean and Keplerian periodograms. *Astron. Astrophys.* **496**, 577. [DOI](#).